Vol. 36, No. 2 (2014) 172-180

Tribology in Industry

www.tribology.fink.rs

RESEARCH

Thermo-mechanical Analysis of the Dry Clutches under Different Boundary Conditions

O.I. Abdullah[a], J. Schlattmann[a], A.M. Al-Shabibi[b]

[a] *System Technology and Mechanical Design Methodology, Hamburg University of Technology, Germany,*
[b] *Department of Mechanical and Industrial Eng. College of Eng. / Sultan Qaboos University.*

Keywords:

Dry friction
Disc clutch
FEM
Thermo-Mechanical behaviour
Temperature field

Corresponding author:

Oday I. Abdullah
System Technology and Mechanical Design Methodology,
Hamburg University of Technology,
Hamburg, Germany.
E-mail: oday.abdullah@tu-harburg.de

A B S T R A C T

The high thermal stresses, generated between the contacting surfaces of the clutch system (pressure plate, clutch disc and flywheel) due to the frictional heating during the slipping, are considered to be one of the main reasons of clutch failure. A finite element technique has been used to study the transient thermoelastic phenomena of a dry clutch. The effect of the boundary conditions on the contact pressure distribution, the temperature field and the heat flux generated along the frictional surfaces are investigated. Analysis has been completed using two dimensional axisymmetric model that was used to simulate the clutch elements. ANSYS software has been used to perform the numerical calculation in this paper.

1. INTRODUCTION

At beginning of the engagement of the clutch disc the slipping will occur between the contact surfaces and the energy will be dissipated by frictional heating, generated at the sliding interface, causing an increase in the surface temperature of the contacting surfaces of the clutch elements (flywheel, clutch disc and pressure plate). The surface temperature and the forces involved are sufficiently to produce non-uniform deformation which affects the pressure distribution and the mating surfaces.

Abdullah and Schlattmann [1-7] investigated the temperature field and the energy dissipated for the dry friction clutch during a single and repeated engagement assuming uniform pressure and uniform wear conditions. They also studied the effect of pressure between contact surface on the temperature field and the internal energy of clutch disc varying with time using two approaches; heat partition ratio approach to compute the heat generated for each part individually whereas the second applies the total heat generated for the whole model using contact model. Furthermore, they studied the effect of engagement time and sliding velocity function, thermal load and dimensionless disc radius (inner disc radius/outer disc radius) on the thermal behaviour of the friction clutch in the beginning of engagement.

2. FINITE ELMENT ANALYSIS

The finite element simulation of the clutch system involves constructing two different models, the first of which is used to solve the thermoelastic problem to yield the displacement field and the contact pressure distribution. The other model is used to solve the transient heat conduction problem to account for the change in the temperature field.

The two models are however coupled since the contact pressure from the first model is needed to define the frictional heat flux in the second model. Furthermore, the temperature field from the heat conduction model is required for the computation of the contact pressure. To account for the coupling and the time variation of the sliding speeds, the clutch engagement time is divided into small time steps. At each time step, the instantaneous nodal temperatures are used in a thermoelastic contact solution to determine the contact pressure distribution. The pressure distribution is assumed to remain constant during the subsequent time. Figure 1 shows the schematic diagram for the finite element simulation of a coupled-field problem of clutches.

Figure 2 shows the interfaces of two adjacent subregions i and j of elastic bodies. The elastic contact problem is treated as quasi-static with standard unilateral contact conditions at the interfaces. The following constraint conditions of displacements are imposed on each interface [8]:

$$w_i = w_j, \quad if \quad P > 0 \tag{1}$$

$$w_i \le w_j, \quad if \quad P = 0 \tag{2}$$

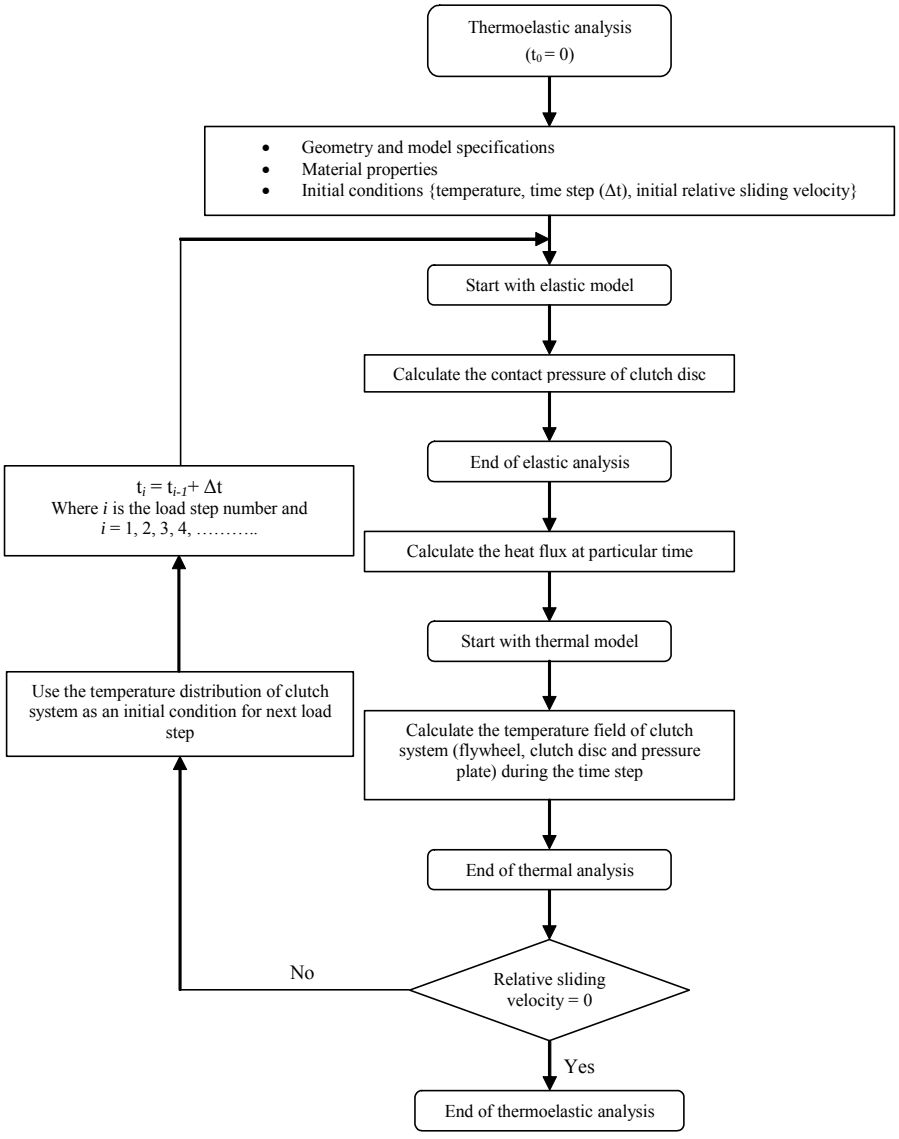

Fig. 1. Schematic diagram of FE simulation.

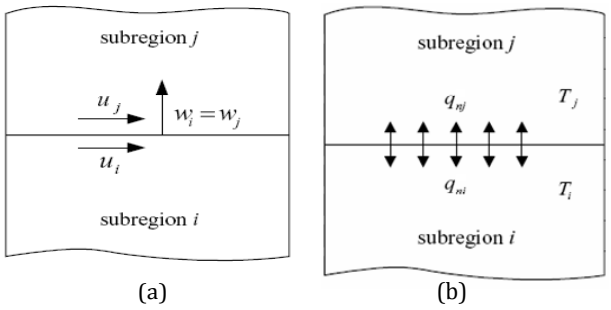

Fig. 2. Contact model for the (a) elastic and (b) heat conduction problem in two adjacent subregions.

Where P is the normal pressure on the friction surfaces. The radial component of the sliding velocity resulting from the deformations is considerably smaller than the circumferential component. Therefore, the frictional forces in radial direction on the friction surfaces are disregarded in this study. Figure 2 (b) shows thermal phenomena of two adjacent subregions of bodies. The interfacial thermal boundary conditions depend on the state of mechanical contact. Two unknown terms q_{ni} and q_{nj} exist on each interface. To fully define the heat transfer problem, two additional conditions are required on each contact interface. If the surfaces are in contact, the temperature continuity condition and the heat balance condition are imposed on each interface:

$$T_i = T_j, \qquad if \;\; P > 0 \tag{3}$$

$$q = \mu P \omega r = -\sum q_n = -(q_{ni} + q_{nj}), if \;\; P > 0 \tag{4}$$

where μ and ω are the coefficients of friction and angular sliding velocity, respectively. Then, using the aforementioned conditions, equations of one node from each pair of contact nodes are removed. If the surfaces are not in contact, the separated surfaces are treated as an adiabatic condition:

$$q = 0 = q_{ni} = q_{nj}, \qquad if \;\; P = 0 \tag{5}$$

Assume the sliding angular velocity decreases linearly with time as:

$$\omega\ (t) = \omega_o (1 - \frac{t}{t_s}), \qquad 0 \le t \le t_s \tag{6}$$

The distribution of the normal pressure P in Eq. (4) can be obtained by solving the mechanical problem occurring in the disc clutch. The first step in this analysis is the modeling; due to the symmetry in the geometry (frictional lining without grooves) and boundary conditions of the friction clutch (taking into consideration the effect of pressure and thermal load due to the slipping), two-dimensional axisymmetric FEM can be used to represent the contact between the clutch elements during the slipping period as shown in Fig. 3. The axisymmetric finite element models (elastic and thermal) of friction clutch system with boundary conditions are shown in Fig. 4. In Fig. 4.a, h is the flow of heat to the surrounding due to convection and $Q_{gen.f}$, $Q_{gen.c}$ and $Q_{gen.p}$ are the amounts of heat flux that enter to the flywheel, clutch disc and pressure plate respectively. Four different cases of boundary conditions are taken into consideration in this work (Fig. 4b-e); restricting two nodes at the backside of flywheel (case-1), restricting all the backside of flywheel (case-2), restricting three nodes (at inner, mean and outer radii) at the backside of flywheel (case-3) and restricting 10 % of the backside of flywheel (case-4). In all computations for the friction clutch model, material has been assumed homogeneous and isotropic and all parameters and material properties are listed in Table 1. Analysis is conducted by assuming there are no cracks in the contact surfaces.

Table 1. The properties of materials and operations.

Parameters	Values
Inner radius of friction material & axial cushion, r_i [m]	0.06298
Outer radius of friction material & axial cushion, ro [m]	0.08721
Thickness of friction material [m], t_l	0.003
Thickness of the axial cushion [m], $t_{axi.}$	0.0015
Inner radius of pressure plate [m], r_{ip}	0.05814
Outer radius of pressure plate [m], r_{op}	0.09205
Thickness of the pressure plate [m], t_p	0.00969
Inner radius of flywheel [m], r_{if}	0.04845
Outer radius of flywheel [m], r_{of}	0.0969
Thickness of the flywheel [m], t_f	0.01938
Pressure, p [MPa]	1
Coefficient of friction, μ	0.2
Number of friction surfaces, n	2
Young's modulus for friction material, E_l [GPa]	0.30
Young's modulus for pressure plate, flywheel & axial cushion, (E_p, E_f, and E_{axi}), [Gpa]	125
Poisson's ratio for friction material,	0.25
Poisson's ratio for pressure plate, flywheel & axial cushion	0.25
Density for friction material, (kg/m^3), ρ_l	2000
Density for pressure plate, flywheel & axial cushion, (kg/m^3), (ρ_p, ρ_f, and ρ_{axi})	7800
Specific heat for friction material, [J/kg K]	120
Specific heat for pressure plate, flywheel & axial cushion, [J/kg K]	532
Conductivity for friction material, [W/mK]	1
Conductivity for pressure plate, flywheel & axial cushion [W/mK]	54
Thermal expansion for friction material and steel [K-1]	12e-6
Slipping time, t_s [s]	0.4

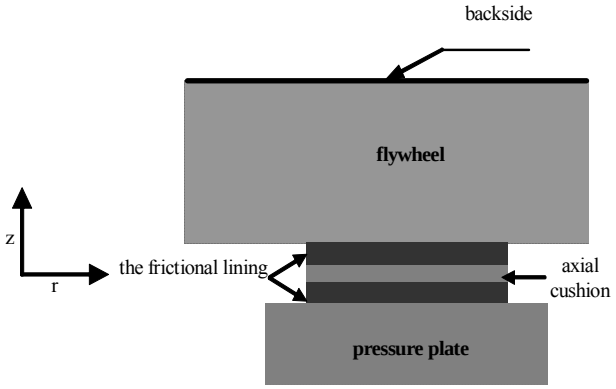

Fig. 3. The Contact model for clutch system.

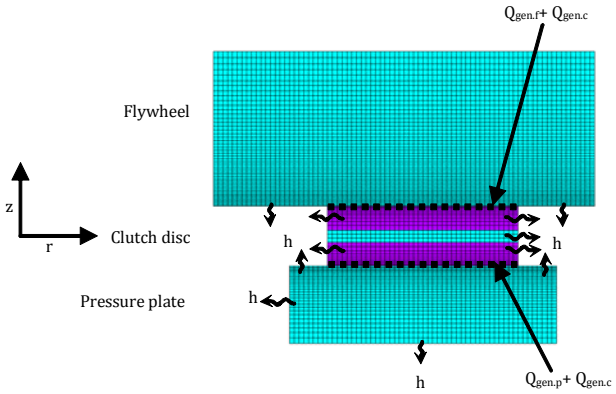

Fig. 4a. FE models with the boundary conditions, (Thermal model).

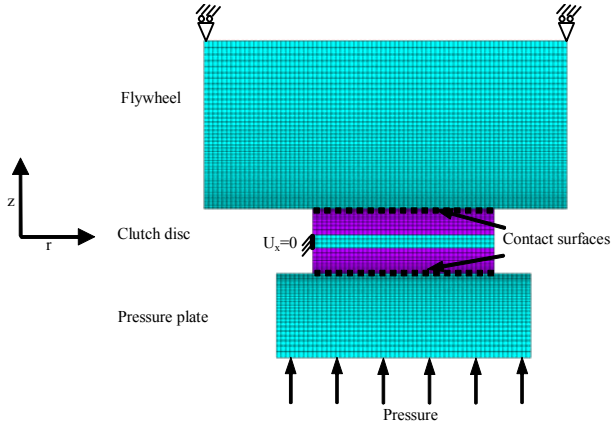

Fig. 4b. FE model with boundary conditions (elastic model, case-1).

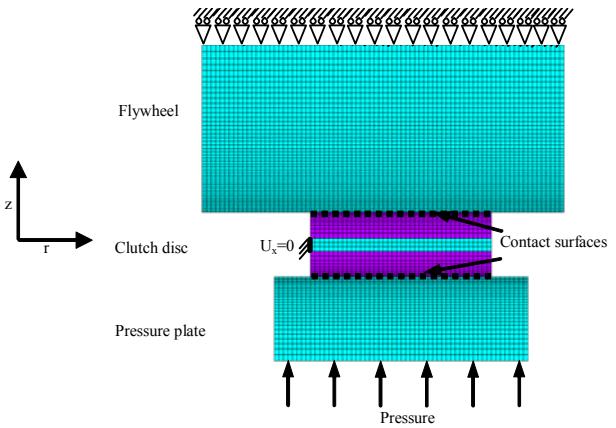

Fig. 4c. FE model with boundary conditions (elastic model, case-2).

3. RESULTS AND DISCUSSIONS

The numerical model is simulated using a finite element method to investigate the effect of boundary conditions on the thermoelastic behavior of clutch system. The simulations consist of two models; the first one is the elastic contact model which is used to calculate the pressure distribution between contact surfaces. The second model is the heat conduction model used to calculate the temperature field during the slipping period.

Figures (5-12) show the contact pressure distribution on the contacting surfaces of both sides of clutch disc (flywheel and pressure plate sides) at selected time intervals (0.12s, 0.24s, 0.36s, 0.4 s). It can be seen from these results that the maximum value of the contact pressure increases with time but in the other side the contact area decreases with time. For both sides of the clutch disc at all time intervals, contact pressure of case-4 is higher than all other cases. In general, pressure distribution on friction surfaces undergoes changes due to thermal deformation which is known as thermoelastic transition. This process of growth of non-uniformity in contact pressure distribution can be unstable and then TEI (thermoelastic instability) phenomenon takes place in the sliding system. The same behaviour of contact pressure for cases (1, 2 and 3) can be observed and the difference between them is very small that can be neglected (less than 0.09%). The maximum values of contact pressure of case-4 are found to be 3.38 MPa and 3.29 MPa corresponding to flywheel and pressure plate sides respectively.

Figures (13-20) demonstrate the variation of the heat flux with clutch disc radius for both sides of clutch disc at selected time intervals. It can be seen, at beginning of the engagement of clutch (t=0.04s), the maximum value of heat flux occurs near ro and the minimum value occurs at ri for all the cases except case-4. It has a different behaviour. The heat flux is semi-uniform for case-4 at this time period. After short time from the beginning of engagement the thermal deformation will affect the contact pressure distribution. So, the heat flux distribution will also change. The heat flux area decreases with time for all the cases but for case-4 the heat flux area is even smaller than the other cases. The maximum values of the heat flux for all the cases occur near the inner radius, and are found to be 7.4 MW/m^2 and 7.44 MW/m^2 corresponding to the flywheel and pressure plate sides respectively.

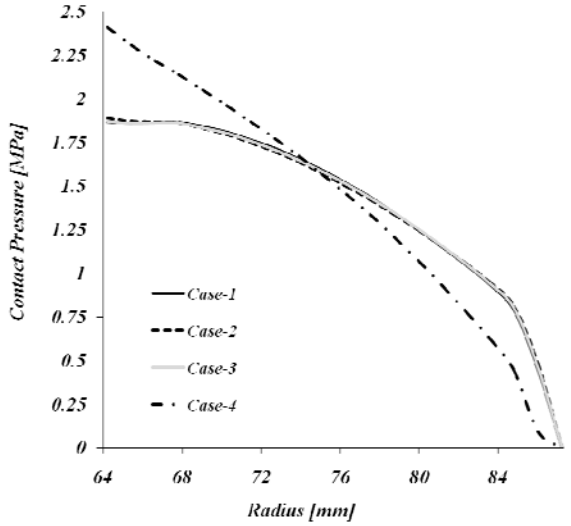

Fig. 5. Contact pressure distribution at flywheel side with different boundary conditions at t = 0.12 s.

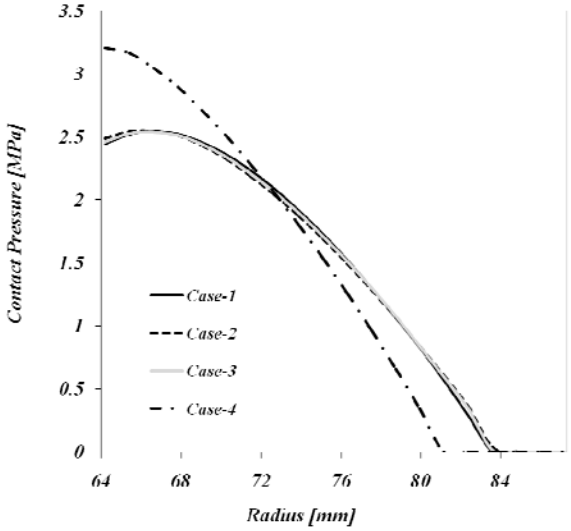

Fig. 6. Contact pressure distribution at flywheel side with different boundary conditions at t = 0.24 s.

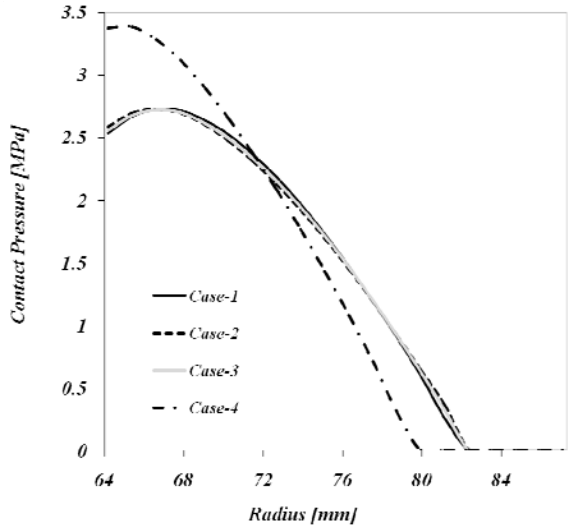

Fig. 7. Contact pressure distribution at flywheel side with different boundary conditions at t = 0.36 s.

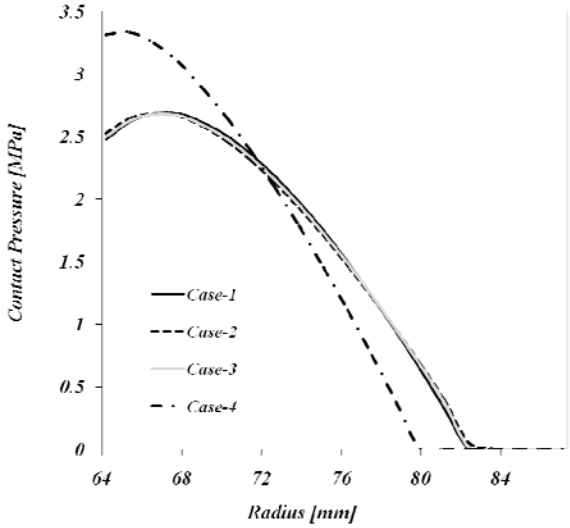

Fig. 8. Contact pressure distribution at flywheel side with different boundary conditions at t = 0.40 s.

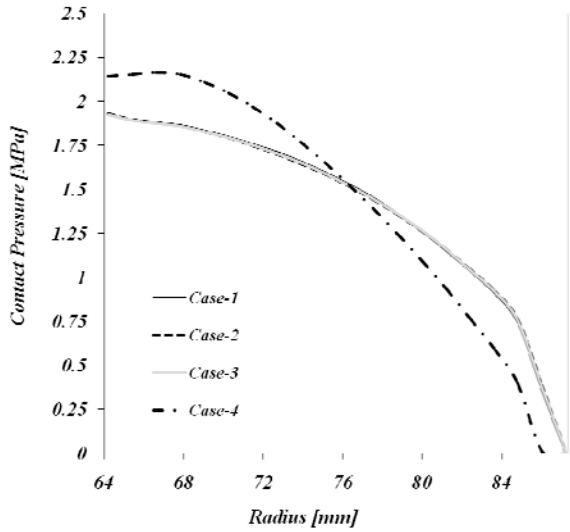

Fig. 9. Contact pressure distribution at pressure plate side with different boundary conditions at t = 0.12 s.

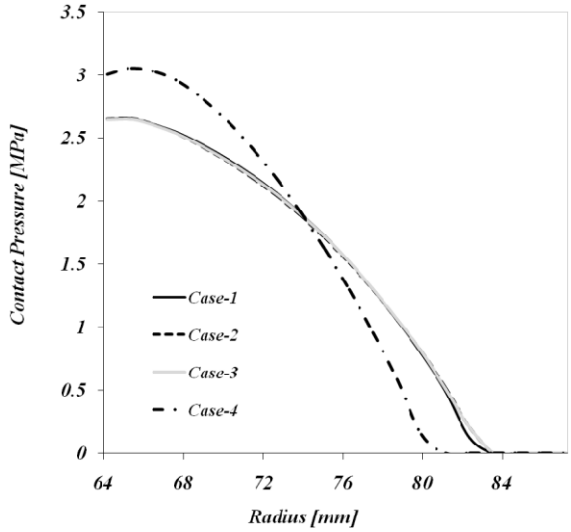

Fig. 10. Contact pressure distribution at pressure plate side with different boundary conditions at t = 0.24 s.

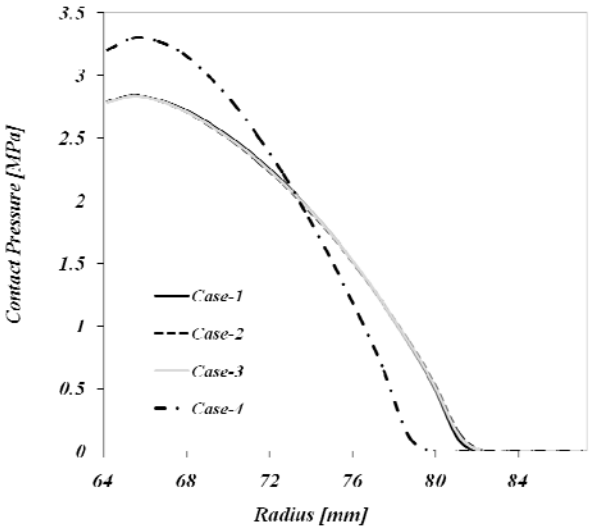

Fig. 11. Contact pressure distribution at pressure plate side with different boundary conditions at t = 0.36 s.

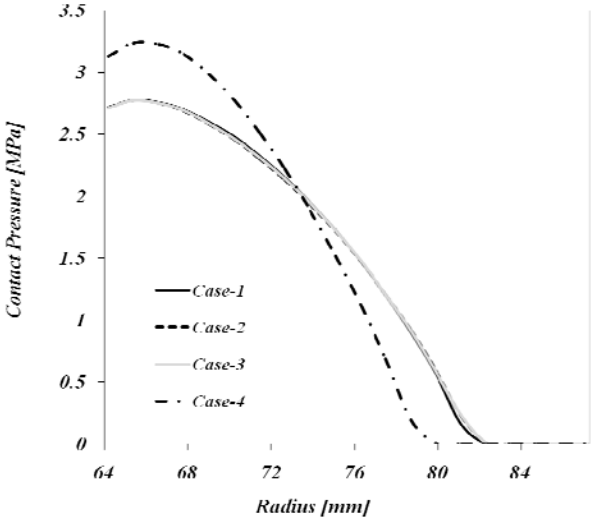

Fig. 12. Contact pressure distribution at pressure plate side with different boundary conditions at t = 0.40 s.

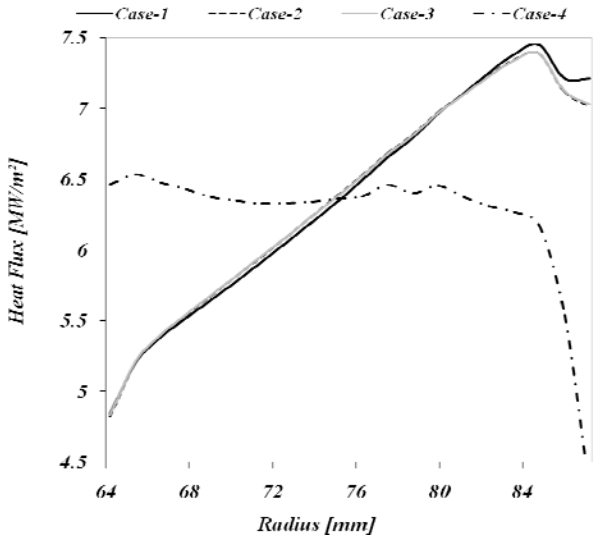

Fig. 13. Heat flux distribution at flywheel side with different boundary conditions at t = 0.04 s.

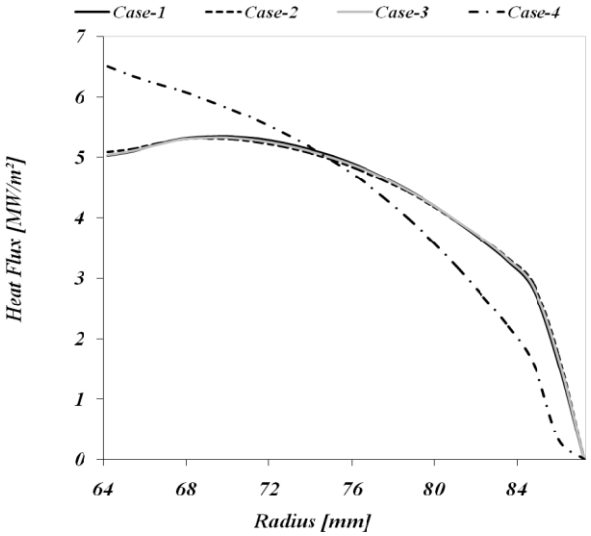

Fig. 14. Heat flux distribution at flywheel side with different boundary conditions at t = 0.16 s.

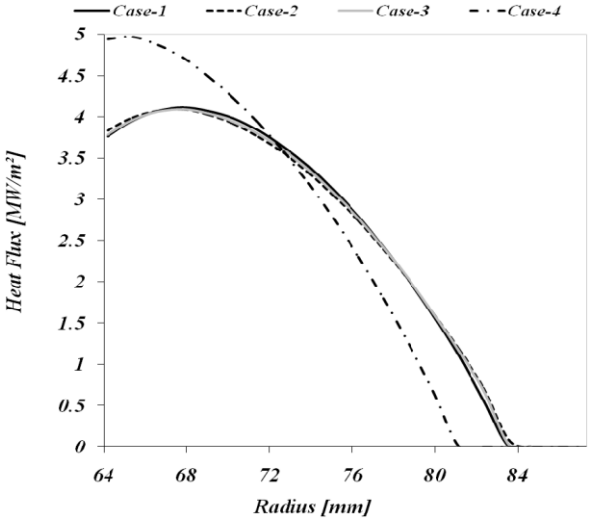

Fig. 15. Heat flux distribution at flywheel side with different boundary conditions at t = 0.28 s.

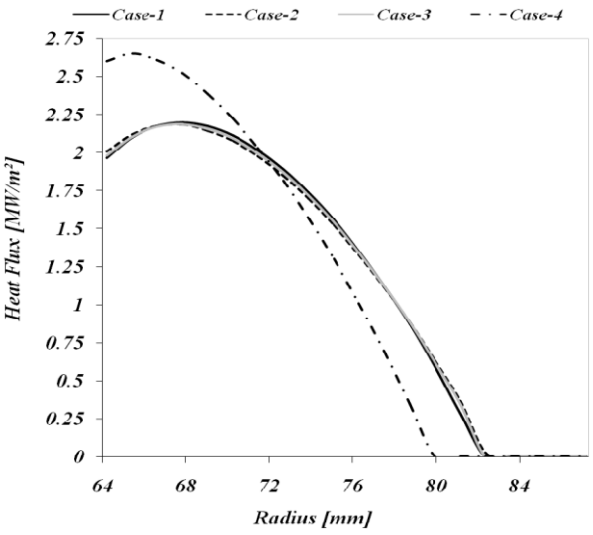

Fig. 16. Heat flux distribution at flywheel side with different boundary conditions at t = 0.36 s.

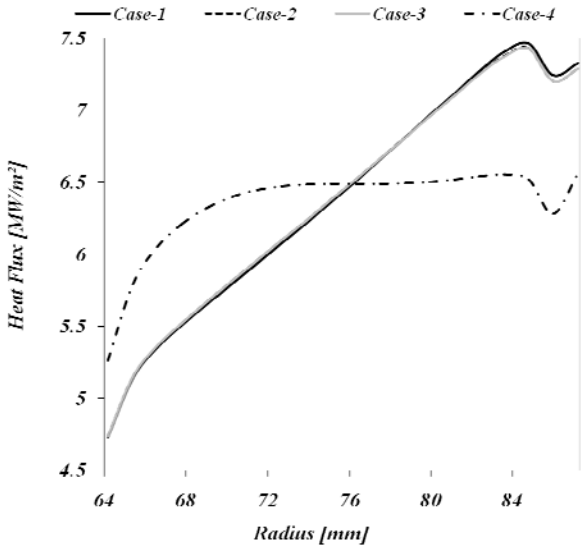

Fig. 17. Heat flux distribution at pressure plate side with different boundary conditions at t = 0.04 s.

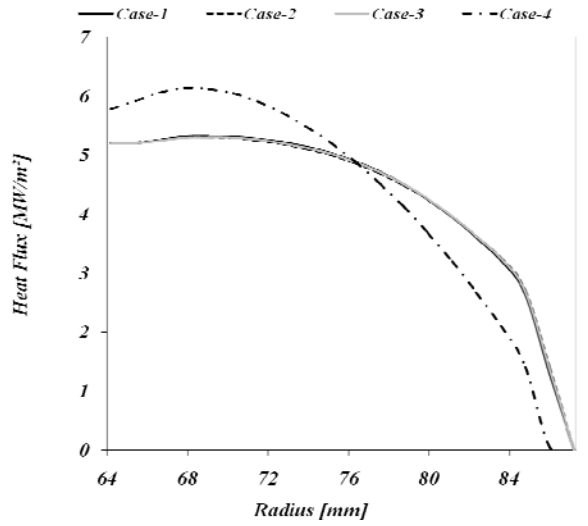

Fig. 18. Heat flux distribution at pressure plate side with different boundary conditions at t = 0.16 s.

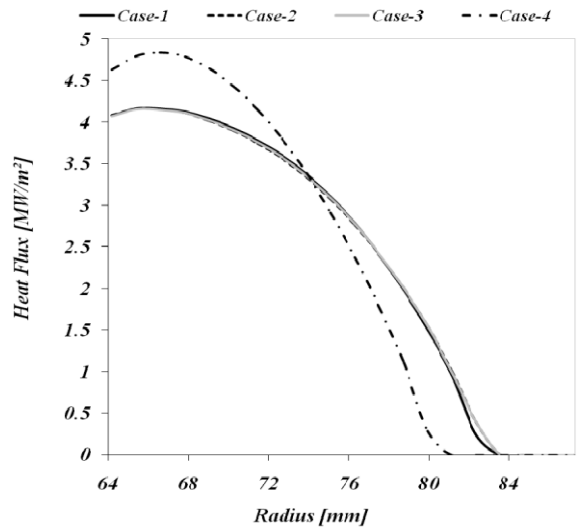

Fig. 19. Heat flux distribution at pressure plate side with different boundary conditions at t = 0.28 s.

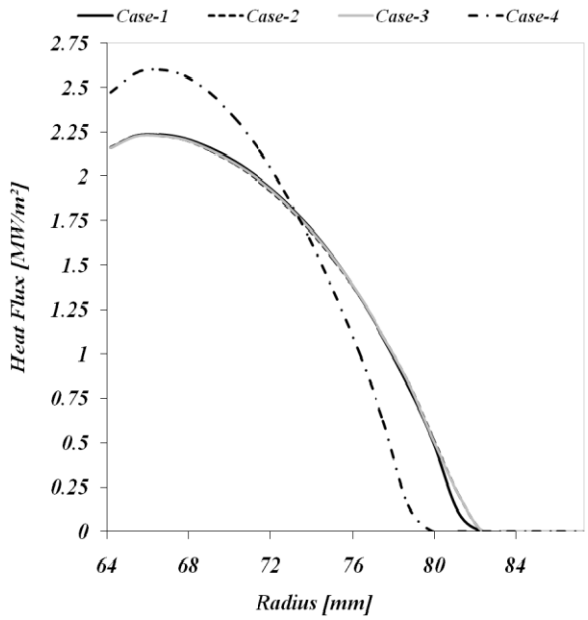

Fig. 20. Heat flux distribution at pressure plate side with different boundary conditions at t = 0.36 s.

Figures (21-24) show the temperature distribution on the friction surfaces of clutch disc at different selected time interval. The temperature distributions on the friction surface for the cases (1, 2 and 3) have the same trend (difference between them is very small and can be neglected). The maximum values of temperature occur at t = 0.24s and are found to be 464.9 K and 489.9 K for cases (1, 2 and 3) and case-4, respectively. The maximum values of temperature occur at r = $0.238r_o$ for all cases.

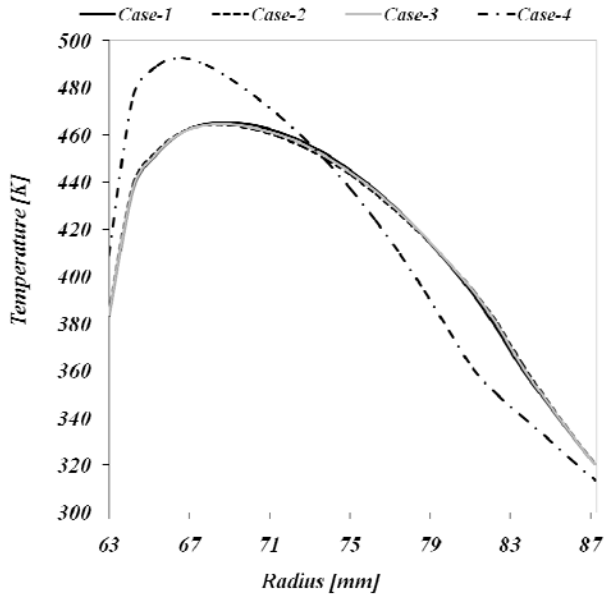

Fig. 21. Temperature distribution along the radius at flywheel side at t = 0.24 s.

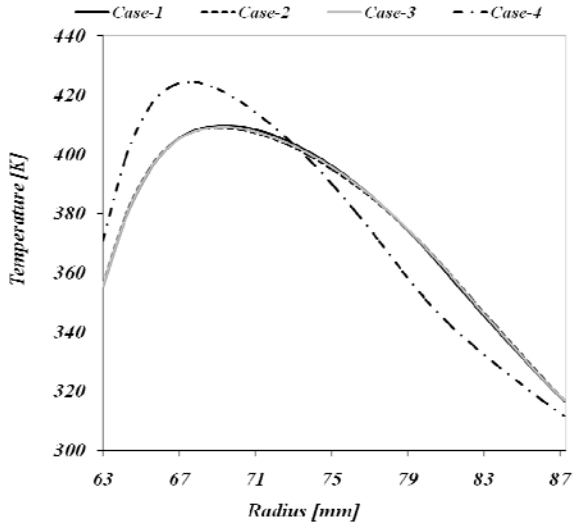

Fig. 22. Temperature distribution along the radius at flywheel side at t = 0.40 s.

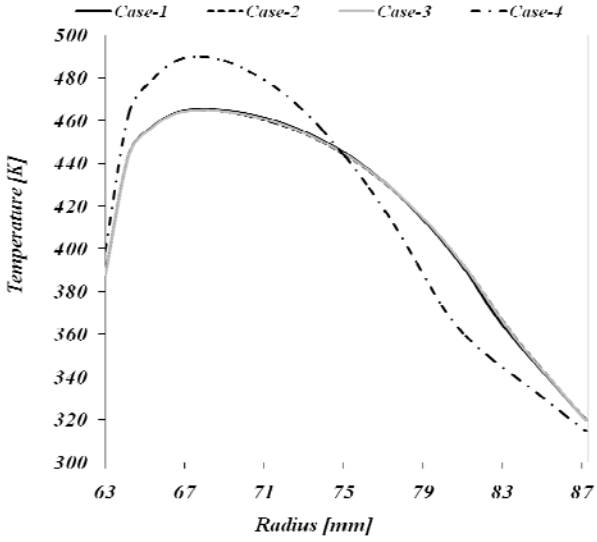

Fig. 23. Temperature distribution along the radius at pressure plate side at t = 0.24 s.

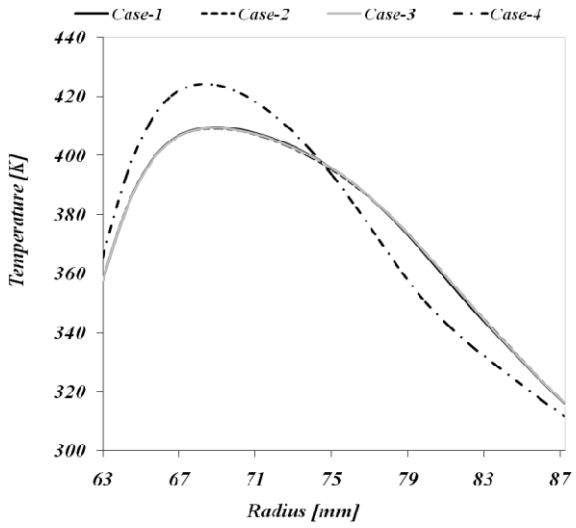

Fig. 24. Temperature distribution along the radius at pressure plate side at t = 0.40 s.

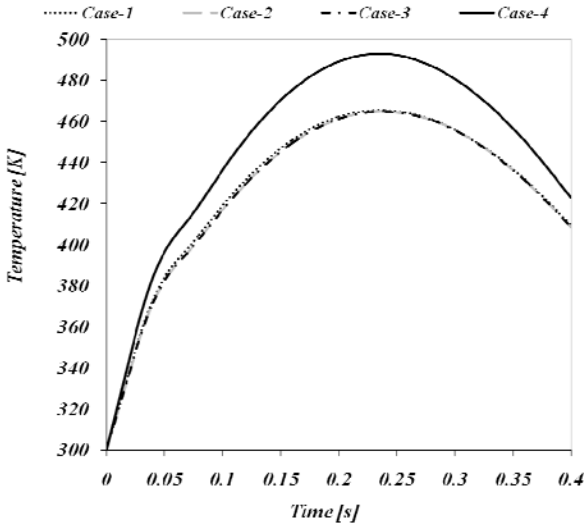

Fig. 25. Maximum temperature history for different boundary conditions of clutch system.

Figure 25 shows the maximum temperature history in the clutch system. The maximum values of temperature occur at t= 0.6ts for all cases. The maximum values of temperature during the slipping period are found to be 465 K and 492.8 K for cases (1, 2 and 3) and case-4, respectively.

4. CONCLUSIONS

In this paper, the transient thermoelastic analysis of clutch system (single disc) has been performed. Two-dimensional thermo-elastic coupling model has been applied to the thermoelastic contact with frictional heat generation. The effect of boundary conditions on thermoelastic behaviour was investigated. The same sliding speed has been assumed for all the cases.

It can be concluded that the thermoelastic behaviour of clutch is affected by the boundary conditions and the magnitude of this affect is more considerable when assuming the boundary condition as case-4. The thermoelastic effect starts in the clutch system at t = 0.05 s. The maximum values of temperature occur in the flywheel side at t ≈ 0.24 s ($0.6t_s$) during the slipping period of 0.4 s. The maximum values of contact pressure occur near the inner radius at t=0.36 s for all the cases. This study presents a valuable design tool, to investigate the effect of boundary conditions on the thermoelastic behaviour of the clutch system during the beginning of its engagement.

REFERENCES

[1] O.I. Abdullah, J. Schlattmann: *"The Effect of Disc Radius on Heat Flux and Temperature Distribution in Friction Clutches",* Journal of Advanced Materials Research, Vol. 505, pp. 154-164, 2012.

[2] O.I. Abdullah, J. Schlattmann: *"Finite Element Analysis of Dry Friction Clutch with Radial and Circumferential Grooves"*, in: *Proceeding of World Academy of Science, Engineering and Technology Conference*, Paris, 2012, pp. 1279-1291.

[3] O.I. Abdullah, J. Schlattmann: *"Effect of Band Contact on the Temperature Distribution for Dry Friction Clutch"*, Tribology in Industry, Vol. 35, No. 4, pp. 317-329, 2013.

[4] O.I. Abdullah, J. Schlattmann: *"The Correction Factor for Rate of Energy Generated in the Friction Clutches under Uniform Pressure Condition"*, Journal of Advances in Theoretical and Applied Mechanics, Vol. 5, No. 6, pp. 277 – 290, 2012.

[5] O.I. Abdullah, J. Schlattmann: *"Finite Element Analysis of Temperature Field in Automotive Dry Friction Clutch"*, Tribology in Industry, Vol. 34, No. 4, pp. 206-216, 2012.

[6] O.I. Abdullah, J. Schlattmann, A.M. Al-Shabibi: *"Transient Thermoelastic Analysis of Multi-disc Clutches"*, in: *Proceedings of 9th Arnold Tross Colloquium*, Hamburg, June 2013.

[7] O.I. Abdullah, J. Schlattmann: *"Stresses and Deformations Analysis of a Dry Friction Clutch System",* Tribology in Industry, Vol. 35, No. 2, pp. 155-162, 2013.

[8] A.M. Al-Shabibi, J.R. Barber: *"Transient Solution of the Unperturbed Thermoelastic Contact Problem"*, Journal of Thermal Stresses, Vol. 32, No. 3, pp. 226-243, 2009.